Numerical study on subcooled boiling and flashing-induced flow instability under rolling motion

YU Shengzhi[1], WANG Jianjun[1], YAN Changqi[1], and GUO Xueqing[1]

1. Fundamental Science on Nuclear Safety and Simulation Technology Laboratory, Harbin Engineering University, Harbin, 150001, China (wang-jianjun@hrbeu.edu.cn, changqi_yan@163.com)

Abstract: The natural circulation system is very important to the designs of the reactor systems with passive safety features. When nuclear powered ship sails on the sea, the natural circulation system may be influenced by the ocean conditions. The typical motions of a ship contain rolling, heaving, pitching, inclination, *etc*. under the ocean condition. In this paper, the mathematical models of the natural circulation system under rolling conditions are presented on the basis of some simplification. The natural circulation characteristics, along with the sub cooled boiling in the heated section and the flashing in the adiabatic riser (the section with up flow where there is no energy exchange with environment.) under rolling motion are studied by self-developed in-house code. The results show that: (1) The oscillating period of intermittent subcooled boiling and flashing-induced flow instability decreases with heat flux increasing when the heated section remains vertical. (2) Under rolling motion condition, the flashing and the sub cooled boiling has been enhanced. (3) The period of the mass flow rate oscillation is about an integeral multiple of the rolling motion period.

Keyword: natural circulation; flashing; sub cooled boiling; rolling motion

1 Introduction

The first nuclear-power submarine launched successfully in the United States in 1954, and then the nuclear power were widely used in the ship and submarine. Affected by the ocean wave, the ship will suffer rolling, heaving and pitching motions.[1-3] The effects of ship motions should be taken into account when concerning the thermal–hydraulic performance of reactor systems in the ship.[1-9] The rolling motion of the ship can change the position of the primary coolant system nonlinearly and introduce the additional inertial force.[7-9] This means that different amplitudes, periods and positions of the rolling motion have different effects in different system compositions. In particular, even for the single phase flow, the experimental and numerical studies proved that in terms of driving pressure head, the ocean condition has more influence in natural circulation system than in forced circulation system.[7-12]

Historically, the study of two-phase flow instabilities started with the pioneering article of Ledinegg[20]. But until several decades later, around 1960s, researchers just began to turn their attention into this kind of phenomena occurring in two-phase flow systems for the development of industrial high-power-density boilers and boiling water reactors (BWR). It is not until late 1960s that the main instability mechanisms were understood, especially due to the development of analytical and computational tools. [13] It was also proven that numerical study is also an effective way to understand mechanisms of some two-phase instabilities. So far, the mechanisms of two-phase instability has been well understood, especially in nuclear industry.[13-14]

However, the influence of rolling motion on flow instability has not been studied in very detail. Tan[9], Guo[15] and Zhang[14] had done some work in this aspect. Meanwhile, under rolling condition, the transient characteristics is a relative universal phenomenon for natural circulation system.[10-12] Therefore, the study of the effects of rolling motion on the flow instability in natural circulation system have the practical significance.

2 Geometrical model

The scheme of the studied natural circulation system is shown in Fig.1, which consists of a heater, a condenser, a pressurizer and connecting pipes. The secondary side of the condenser is operated in a

Received date: May 2, 2016
(Revised date: July 13, 2016)

forced circulation way. All of the components of the primary natural circulation loop are fixed on the rolling platform. Some of the system geometrical parameters are listed in Table 1.

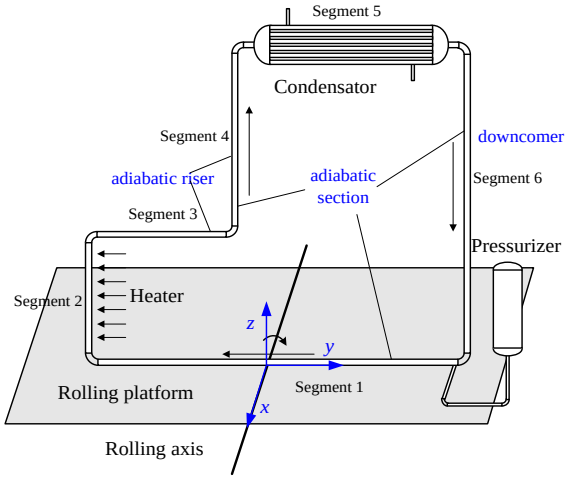

Fig. 1 Scheme of the closed natural circulation system.

Table 1 Geometrical parameters of the natural circulation loop

parameter	value
Pressurizer initial pressure (MPa)	0.15
Length of condenser (m)	0.9
The coolant velocity in secondary side of condenser (m/s)	3.0
The coolant temperature (inlet) in secondary side of condenser (℃)	30.0
Heat transfer area of condenser (m^2)	0.006283
Length of heater (m)	1.0
Height difference between the heat exchanger and condenser (m)	2.0
Heat transfer area of heater segment (m^2)	0.00212
Heat flux of heater(kW/m^2)	50 or 60
Initial water temperature in primary loop (℃)	30.0

Table 2 the position coordinates on the rolling platform

parameter	*From* (m)	*To* (m)
Segment 1	(0.0, 1.0, 0.0)	(0.0, -1.0, 0.0)
Segment 2	(0.0, -1.0, 0.0)	(0.0, -1.0, 1.0)
Segment 3	(0.0, -1.0, 1.0)	(0.0, 0.0, 1.0)
Segment 4	(0.0, 0.0, 1.0)	(0.0, 0.0, 3.0)
Segment 5	(0.0, 0.0, 3.0)	(0.0, 1.0, 3.0)
Segment 6	(0.0, 1.0, 3.0)	(0.0, 1.0, 0.0)

Under rolling motion condition, the flow rate of natural circulation is not only affected by the geometric structure of primary loop but also the location relative to rolling axis. In order to present the relative arrangement of the components in detail, Table 2 shows the position coordinates of the loop components on the rolling platform. It is worthy to note that the Cartesian coordinate system was built on rolling plane as shown in Fig.1.

3 Numerical model

3.1 The basic assumptions

A one-dimensional computational code is developed to investigate the operation behaviors of the natural circulation loop under rolling condition based on the non-equilibrium model for two-phase flow. Several assumptions are made as follows:

1) All the connecting pipes are adiabatic.
2) The saturation parameters, *e.g.* saturation enthalpy, saturation density and saturation temperature, are supposed to depend on the local pressure along the channel. The other state parameters are dependent on the local pressures and temperatures.
3) The axial heat conduction along the heated section is not going to be considered.
4) The steam always keeps in saturation state.

3.2 The rolling condition simulation

It is usually assumed that the rolling motion is in a sinusoidal order.[19] The rolling angular velocity and angular acceleration could be expressed as:

$$\theta=\theta_{\mathrm{m}}\sin(\frac{2\pi}{T}t) \tag{1}$$

$$\omega=\theta_{\mathrm{m}}(\frac{2\pi}{T})\cos(\frac{2\pi}{T}t) \tag{2}$$

So, there is

$$\beta=-\theta_{\mathrm{m}}(\frac{2\pi}{T})^2\sin(\frac{2\pi}{T}t) \tag{3}$$

θ denotes the angle between where the rolling platform is and its balance position during rolling motion. The positive direction of angle is indicated in Fig.1.

Gao *et al.*[7] analyzed the forces acting on coolant under rolling condition, proved the existence of additional acceleration and gave its theoretical expression.

$$\vec{a}_{roll}=-\vec{\omega}\times\left(\vec{\omega}\times\vec{r}\right)-\vec{\beta}\times\vec{r}+\left(2\vec{\omega}\times\vec{u}\right) \tag{4}$$

So, with the assumptions of one-dimensional flow, the additional acceleration can be derived through the vector calculation.

$$a_{pro}=\vec{a}_{roll}\cdot\vec{z} \tag{5}$$

Meanwhile, for the Cartesian coordinate system built on the rolling platform, the acceleration of gravity should take such forms through the vector calculation as (6) and (7).

$$\vec{g} = g\left[\sin\theta, \cos\theta\right] \tag{6}$$

$$g_{pro} = \vec{g} \cdot \vec{z} \tag{7}$$

3.3 The conservation equation & the constitutive relation

The basic mathematic model consists of mass, momentum and energy conservation equations:

$$\frac{\partial W}{\partial z} = 0 \tag{8}$$

$$\frac{\partial \rho u}{\partial t} + \rho u \frac{\partial u}{\partial z} = -\frac{\partial p}{\partial z} - \rho(g_{partial} + a_{roll}) - (\frac{\partial p}{\partial z})_{fri} - (\frac{\partial p}{\partial z})_{local} \tag{9}$$

$$\frac{\partial(\alpha\rho_g i_g + (1-\alpha)\rho_f i_f)}{\partial t} + G\frac{\partial(i_m)}{\partial z} = \frac{q_l}{A} + \frac{\partial P}{\partial t} \tag{10}$$

$$\frac{\partial \alpha\rho_g}{\partial t} + \frac{\partial \alpha\rho_g u_g}{\partial z} = \tau_{sub} + \tau_{con} \tag{11}$$

Where W is the mass flow rate, **kg/s**; A is the area of the cross section for the fluid flow, $\mathbf{m^2}$; i_m is the specific enthalpy of the mixture, **kJ/kg**; q_l is the linear power of source or sink, **W/m**. In the heat exchanger, q_l can be calculated by the transient heat transfer equation. In the adiabatic section, q_l is equal to 0.

If the system operates under two-phase conditions, the parameters in the conservative equations can be defined as follows:

$$W = (\alpha\rho_g u_g + (1-\alpha)\rho_f u_f)A = \rho_o u_m A = GA \tag{12}$$

$$\rho_o = \alpha\rho_g + (1-\alpha)\rho_f \tag{13}$$

$$i_m = x i_g + (1-x) i_f \tag{14}$$

$$u_m = \frac{\alpha\rho_g u_g + (1-\alpha)\rho_f u_f}{\rho_o} \tag{15}$$

The void fraction is calculated such by Bankoff model as formulas (16) and (17).

$$\alpha = K\gamma \tag{16}$$

$$K = 0.71 + 1.45\times10^{-8} p \tag{17}$$

The heat transfer process in heat exchanger is composed of three separate processes, *i.e.*, the heat transfer between fluid in secondary loop and the outer wall of the tubes, the conduction through the tube, and the convection heat transfer between the fluid and inner surface of the tubes:

$$\begin{cases} Q_{out} = Q_{source} & in\ heater \\ Q_{out} = h_{out}\pi D_{out}(T_{w,out} - T_{f,out}) & in\ condensator \end{cases} \tag{18}$$

$$Q_l = h_{in}\pi D_{in}(T_{w,in} - T_{f,in}) \tag{19}$$

The thermal storage of the tubes' wall should be considered in the transient calculation, and every heat structure has 5 intervals in radial direction in calculation.

$$\rho_w c_{p,w}\frac{\partial T_w}{\partial t} = \frac{1}{r}\frac{\partial}{\partial r}\left(r\kappa_w\frac{\partial T_w}{\partial r}\right) \tag{20}$$

3.4 The calculation of heat transfer

If phase change does not occur inside the heat transfer tube, the heat transfer coefficient inside the tube is calculated by formula (21). In addition, the subcooled boiling heat transfer coefficient is predicted by the formula (22) developed by Rosenow, and the saturation boiling heat transfer coefficient is predicted by the formula developed by Chen[21]. The condensation heat transfer coefficient is predicted by the formula developed by Shah[18].

1) The heat transfer coefficient of single phase

$$Nu = \begin{cases} 3.66 & Re \le 2000 \\ 0.023Re^{0.8}Pr^{0.33} & Re > 2000 \end{cases} \tag{21}$$

2) The subcooled boiling heat transfer coefficient

$$\frac{c_{p,f}\Delta T_{sat}}{i_{fg}} = C_{sf}\left[\frac{q_{sub}}{\mu_f i_{fg}}\sqrt{\frac{\sigma}{g(\rho_f - \rho_g)}}\right]^{0.33}\left(\frac{c_{p,f}\mu_f}{\kappa_f}\right)^{1.7} \tag{22}$$

3) The saturation boiling heat transfer coefficient

$$h_{TP} = h_{mac} + h_{mic} \tag{23}$$

Where h_{mac} is the convection heat transfer coefficient, namely, macroscopic heat transfer coefficient; the h_{mic} is the nuclear boil heat transfer coefficient, namely, microscopic heat transfer coefficient.

And there is,

a) $$h_{mac} = 0.023F\left[\frac{G(1-x)d}{\mu_f}\right]^{0.6}(\mathrm{Pr}_f)^{0.4}\frac{\kappa_f}{d} \tag{24}$$

$$F = \begin{cases} 1.0 & X_{tt}^{-1} \le 0.10 \\ 2.35\left(\frac{1}{X_{tt}} + 0.213\right)^{0.736} & X_{tt}^{-1} > 0.10 \end{cases} \tag{25}$$

$$X_{tt} = \left(\frac{1-x}{x}\right)^{0.9}\left(\frac{\rho_g}{\rho_f}\right)^{0.5}\left(\frac{\mu_f}{\mu_g}\right)^{0.1} \tag{26}$$

b) $$h_{mic} = 0.00122\left[\frac{\kappa_f^{0.79}c_{p,f}^{0.45}r_f^{0.49}}{\sigma^{0.5}m_f^{0.29}i_{fg}^{0.24}\rho_g^{0.24}}\right]\Delta T_{sat}^{0.24}\Delta p_{sat}^{0.75}S \tag{27}$$

$$S = \begin{cases} \left[1 + 0.12\left(Re_{TP}^{'}\right)^{1.14}\right]^{-1} & Re_{TP}^{'} < 32.5 \\ \left[1 + 0.42\left(Re_{TP}^{'}\right)^{0.78}\right]^{-1} & 32.5 \le Re_{TP}^{'} \le 70 \\ 0.1 & Re_{TP}^{'} > 70 \end{cases} \tag{28}$$

$$Re_{TP}^{'} = \left(\frac{G(1-x)D}{\mu_f}\right)F^{1.25}\times10^{-4} \tag{29}$$

4) The condensation heat transfer coefficient

$$h_{TP} = h_L\left[(1-x)^{0.8} + \frac{3.8x^{0.76}(1-x)^{0.04}}{p_r^{0.36}}\right] \quad (30)$$

where,

$$p_r = \frac{p}{p_{critical}} = \frac{p}{22.046} \quad (31)$$

For flow boiling, the prediction of the onset point in boiling channel is considered through empirical model or semi-empirical model. The ONB (Onset of Nuclear Boiling), is predicted by the formula developed by Thom. And the FDB (Fully Developed Boiling) is predicted by the formula developed by Saha & Zuber.

ONB (Thom)

$$\Delta T_{sat} = 22.65q^{0.5}\exp(-\frac{p}{8.7}) \quad (32)$$

FDB (Saha & Zuber)

when

$Pe \le 70000$

$$\Delta T_{sub} = 0.0022\frac{qD_e}{\lambda} \quad (33)$$

$Pe > 70000$

$$\Delta T_{sub} = 154\frac{q}{Gc_{p,f}} \quad (34)$$

Where

$$Pe = Re \cdot Pr$$

3.5 The calculation of resistance

The flow resistances along the channel consist of frictional pressure drop, gravitational pressure drop, acceleration pressure drop and local pressure drop.

Frictional pressure resistance of the single-phase flow can be estimated by (35):

$$\left(\frac{\partial p}{\partial z}\right)_{fri} = \frac{\lambda}{D_e}\frac{G^2}{2\rho_m} \quad (35)$$

where, λ is the frictional resistance coefficient,

$$\lambda = \begin{cases} 64Re^{-1} & Re \le 2000 \\ 0.3164Re^{-0.25} & 4000 < Re < 3.0\times10^4 \\ 0.184Re^{-0.2} & Re \ge 3.0\times10^4 \end{cases} \quad (36)$$

Frictional pressure resistance of the two-phase flow is calculated by homogeneous equilibrium model.

$$\left(\frac{\partial p}{\partial z}\right)_{fri} = \phi_{lo}^2\frac{\lambda}{D}\frac{G^2}{2\rho_m} \quad (37)$$

And the ρ_m is the flow density,

$$\rho_m = \frac{1}{v_m} = \frac{1}{xv_g + (1-x)v_f} \quad (38)$$

Where, ϕ_{l0}^2 is the two-phase frictional multiplier,

$$\phi_{l0}^2 = \left[1 + x\left(\frac{\rho_f}{\rho_g} - 1\right)\right] \quad (39)$$

Gravitational pressure drop:

$$\left(\frac{\partial p}{\partial z}\right)_{gra} = \rho_o g \quad (40)$$

Acceleration pressure resistance for two-phase flow:

$$\left(\frac{\partial p}{\partial z}\right)_{acc} = G^2\frac{dv_m}{dz} \quad (41)$$

For the closed loop, the integration of acceleration pressure resistance along loop is zero.

Where

$$\oint_{loop}\left(\frac{\partial p}{\partial z}\right)_{acc} dz = 0 \quad (42)$$

Local pressure resistance:

$$\left(\frac{\partial p}{\partial z}\right)_{loc} = \xi\frac{G^2}{2\rho_m} \quad (43)$$

The explicit numerical integration method is employed in this study. It has been shown that the explicit method of integration has always far less numerical damping than the implicit Euler method even for the same Courant number [17]. And the logic diagram for simulation is shown in Fig.2.

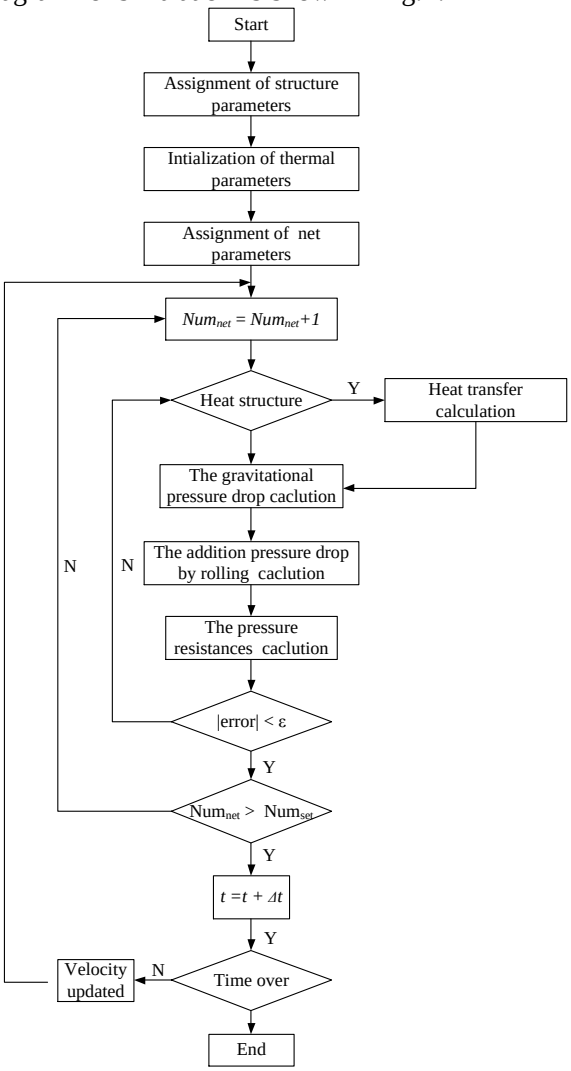

Fig.2 The logic diagram for simulation.

4 Results and discussions

4.1 Sub cooled boiling and flashing-induced flow instability under vertical condition

Before the system is activated, the system is in stationary state and all the pipes are filled with water of 30**°C**. The temperature of the water in secondary loop is 30 **°C**, and the velocity of the water is 3 **m/s**. The initial heat flux of the heated section is zero. With the time increases, the linear heat flux is increasing and reaches to 50 (60 in case2) **kW/m²**. The pump is used to drive the fluid flow in initial stage to accelerate the response of system startup and is shut down after the startup.

4.1.1 Result and discussion under case 1 condition

In case 1, the heat flux of the heated section is 50 **kW/m²**. And the evolutions of mass flow rate and the axial temperature of inner wall of the heated section are depicted in Fig.3. Figure 4 depicts the axial distribution of void fraction verse advancement time. In Fig.3, node 73 indicates the temperature node on the inner wall of heat structure, the distance between this node and the exit of the heated section is 0.10 **m**. The distance for node 74 and 75 respectively are 0.06 **m** and 0.02 **m**.

Several stages with different types of characteristics in per oscillation period can be observed after the system flow instability has been fully developed: subcooled boiling process (A), subcooled boiling and flashing driven transition process (B), flashing driven process (C) and single-phase driven process (D).

It can be easily found in the results shown in Fig.3 that the period of the oscillation is about 47.1 **s**. Combining the dada of Fig.3 and Fig.4, the duration of each stage in per oscillation period can be obtained, respectively 29.0 **s**, 2.0 **s**, 11.3 **s**, and 4.8 **s**.

In stage A of each period of the oscillation, because the mass flow rate is relatively low, the fluid cannot remove all the heat added into the heated section, the inner wall temperature increase as Fig.3 shows. After a short period of time, the FDB is first emerged at the exit of the heated section, for example, in the zone around node 75. Meanwhile, the extent of the FDB starts to move toward the upstream. Due to the boiling phenomenon, the mass flow rate starts to oscillate. In stage B, the heated fluid with relative high temperature moves to the adiabatic riser, the flashing of the fluid may occur when the fluid temperature is higher than the local saturated temperature. From Fig.4, it also can be observed that the onset of flashing first appears at the exit of the riser, which is mainly due to the lower local pressure. In stage C, the flashing process is relatively fully developed and produces a high driven pressure head for the natural circulation system, which makes the mass flow rate rapidly increased. In the meantime, the FDB in heated section is going to die away gradually due to the improvement of the cooling condition. In stage D, the flashing phenomenon disappears and the system operates in single phase mode. With the wearing off of the boiling process, the fluid temperature gradually decreases to be lower than the local saturated temperature at the exit of the riser. Therefore, the flashing stops. During this process, the mass flow rate of the system continues to decrease due to the continuous decrease of the driving force.

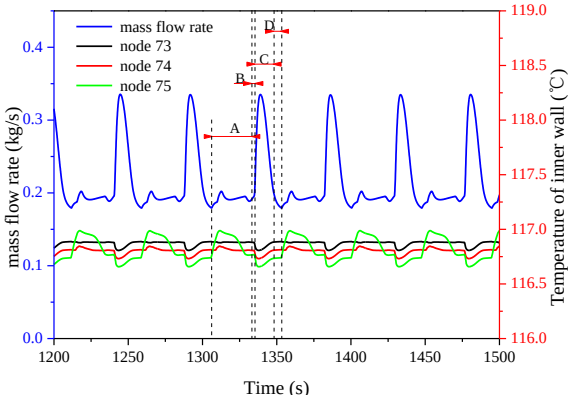

Fig. 3 The mass flow rate and the temperature of partial heater inner wall in flow instability phase.

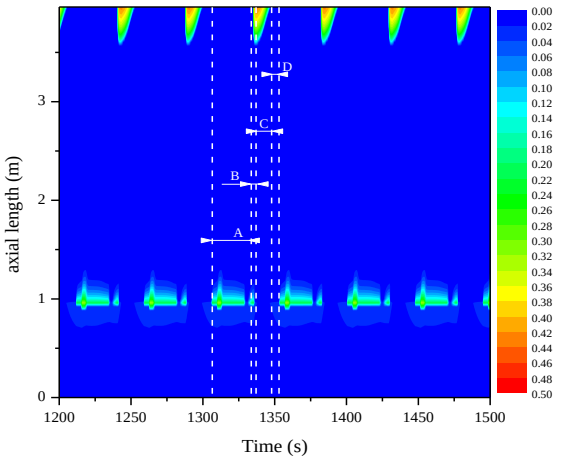

Fig. 4 The axial distribution of void fraction variation with time increase.

4.1.2 Result and discussion under case 2 condition

Figure 5 and Figure 6 have depicted the variation of the mass flow rate, the inner wall temperature and the void fraction axial distribution versus time when the heat flux is 60 **kW/m^2**. Similar to case 1, it also appears intermittent subcooled boiling and flashing in per oscillation period. And there are also four similar stages in per period, but their durations have changed. In this case, they respectively direct 20.7 **s**, 1.9 **s**, 8.6 **s** and 3.1 **s**. It can be observed that the oscillation period gets shorter with the increase of heat flux. Comparing the duration of every stage in two cases, it can be found that the duration time span of stage A and stage D are obviously decreased. It can be explained that the required storage time for flashing decreases with the increase of heat flux.

4.2 Subcooled boiling and flashing-induced flow instability under rolling condition

Under rolling condition, the system is suffering additional inertia force which is caused by rolling motion. It needs to be noted that the interaction between the additional inertia force and the driving force of the loop may influence the behavior of the system. The additional inertia force is somehow forced and can persistently exert an influence on the driving force of the loop. Therefore, the period of the flow instability will intend to be the integer times of rolling motion period, while the times also have an influence on the density wave oscillation period.

In the cases studied, the rolling period and amplitude are 16 **s** and 10 °respectively. And at 1500.0 seconds, the rolling motion starts up.

4.2.1 Result and discussion under case 3 condition

Figure 7 depicts the time series of mass flow rate under the same condition as case 1 except for the rolling motion. It can be found in the results that there is an obvious period which complies with the period of rolling motion. Although the period is about 47.1 s for the density wave oscillation without rolling, the period of the flow instability under rolling condition turns to 32.0 s. The period of the oscillation has been forced to be twice of the period of rolling motion.

Figure 8 presents the axial distribution of void fraction under rolling condition. It can be observed that stage A and stage D occur one by one. It also can be noticed that stage C has been influenced, whose period has been extended.

4.2.2 Result and discussion under case 4 condition

Figure 9 depicts the mass flow rate under rolling motion under the same condition as case 2 but the rolling motion condition. Similar results are derived as case 3. For example, the maximum of the mass flow rate has increased. It can be concluded that the flashing has been enhanced by rolling condition, as well as the subcooled boiling, as shown in Fig.10. But in case 4, the period of mass flow rate has turned to 128.0 s, which is 8 times period of rolling motion. It is different from case 3. But it also can conclude that an integral number of rolling periods fit into the mass flow rate period under rolling condition.

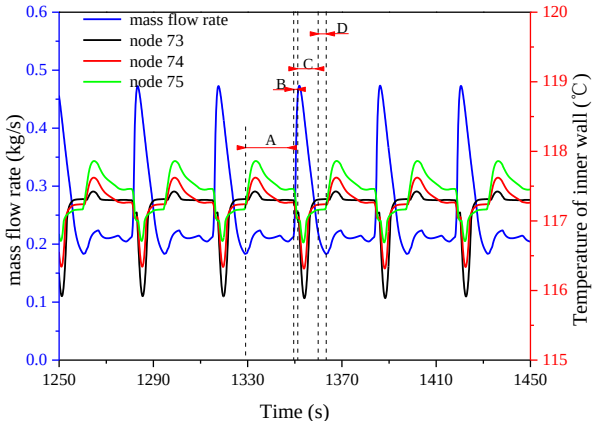

Fig. 5 The mass flow rate and the temperature of partial heater inner wall in flow instability phase.

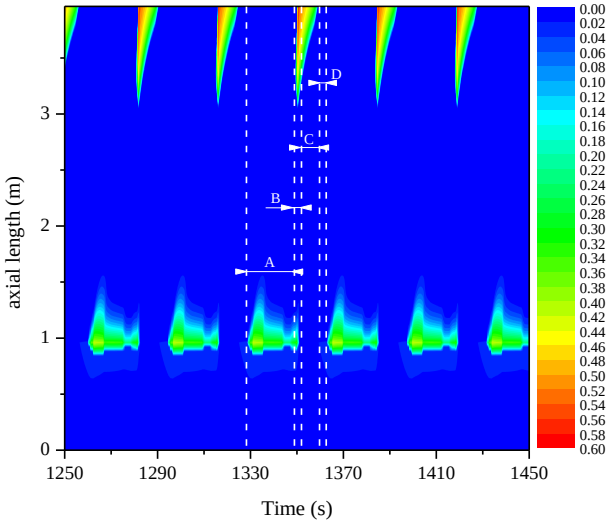

Fig. 6 The axial distribution of void fraction variation with time increase.

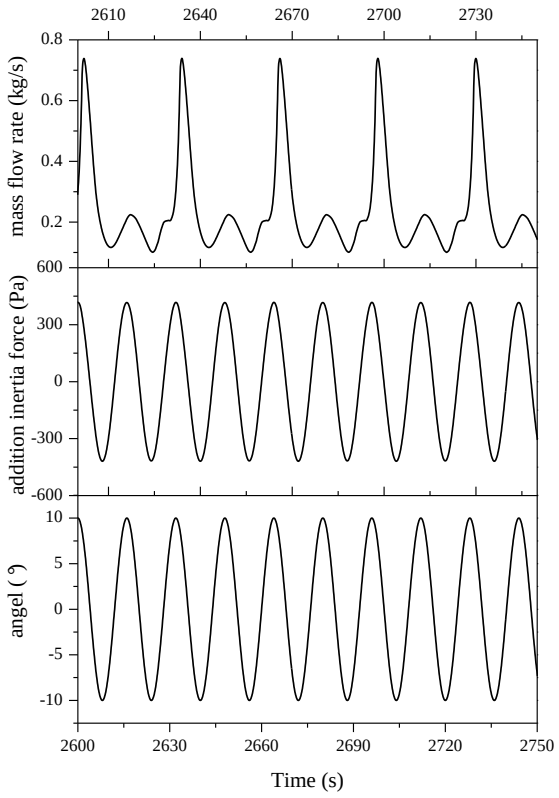

Fig. 7 Mass flow rate under rolling motion condition.

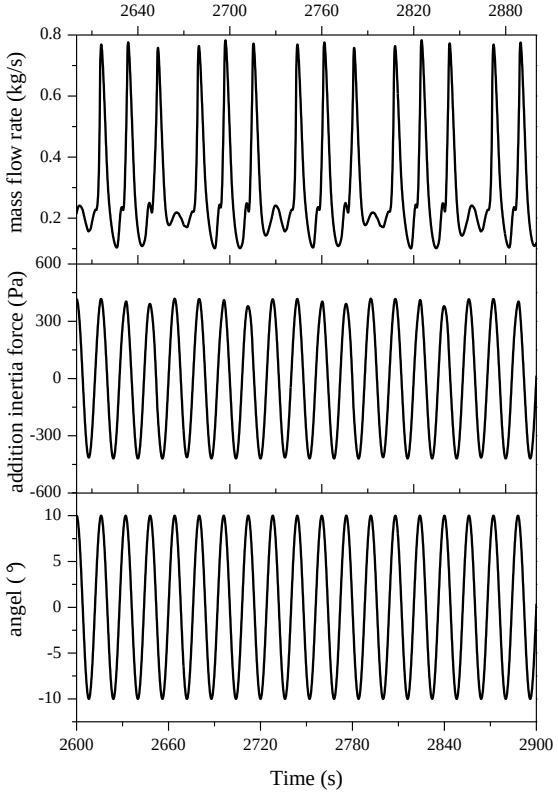

Fig. 9 Mass flow rate under rolling motion condition.

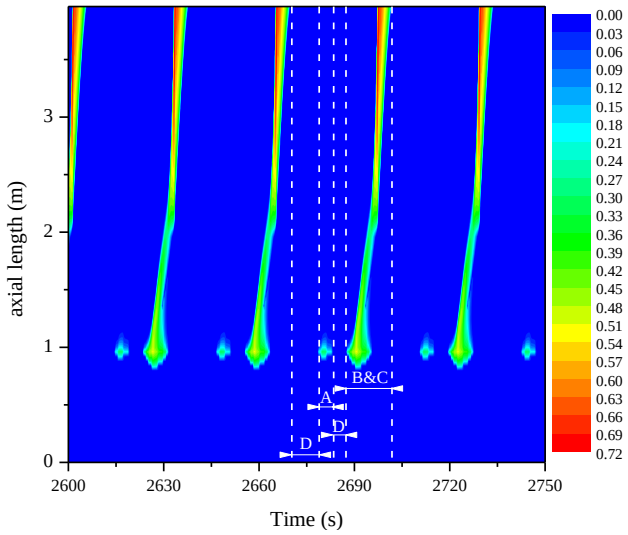

Fig. 8 The axial distribution of void fraction variation under rolling condition.

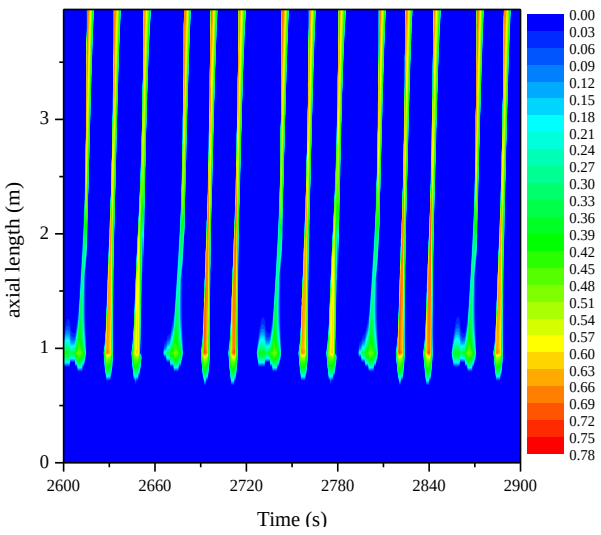

Fig. 10 The axial distribution of void fraction variation under rolling condition.

5 Conclusions

A numerical model based on non-equilibrium model is developed to simulate the transient flow behaviors of subcooled boiling and flashing-induced flow instability under both static and rolling conditions for a natural circulation system. And the effects of rolling motion on the flow characteristics are analyzed. The conclusions are shown as follows:

1. Under the static condition, the oscillating period of intermittent subcooled boiling and flashing-induced flow instability decreases with the increase of the heat flux.
2. Under the rolling condition, the flashing and the subcooled boiling could be enhanced.
3. The rolling motion may exert forced effects on the period of the oscillation occurring in the system, which makes the period of the oscillation to be an integral multiple of rolling motion period.

In future, we plan to verify self-developed simulation code with the experimental results. After that, more studies will be carried out on effects of rolling motion on other instabilities.

Nomenclature

General symbols

W	mass flow rate (kg/s)
G	mass flux (kg/m^2)
v	specific volume (m^3/kg)
u	velocity (m/s)
T	temperature (℃)
$\bar{T}$	rolling period
p	pressure (Pa)
x	mass quantity
t	time (s)
i	specific enthalpy
h	heat transfer coefficient
A	area (m^2)
q	heat flux (W/m^2)
Q	power (W)
D	hydraulic diameter (m)
a	acceleration (m^2/s)
g	gravitational acceleration (m^2/s)
Nu	Nusselt number
Re	Reynolds number
Pe	Berkely number
Pr	Prandtl number
c_p	specific heat at constant pressure (J/(kg·K))

Superscripts

$\rightarrow$	Vector

Greek letters

θ	rolling angle (°)
ω	angular velocity (rad/s)
β	angular acceleration (rad/s^2)
ρ	density (kg/m^3)
α	void fraction
μ	dynamic viscous (Pa·s)
λ	single-phase friction factor
σ	surface tension (N/m)
τ	liquid, vapor generation term (kg/s·m^3)
ξ	local resistance coefficient
γ	volume void fraction

Subscripts

roll	under rolling condition
pro	product of vector
g	gas phase
f	fluid (liquid) phase
m	Mixture
o	real density
fri	friction
loc	Local
acc	acceleration
mic	microsmic
mac	macrosmic
TP	two phase
sub	subcooled
sat	saturation
w	wall
lo	liquid phase flows only through the same pipe with total mass flow rate

Acknowledgments

The authors also gratefully thank for the support of National Natural Science Foundation of China (11175050), Key Laboratory of Advanced Reactor Engineering and Safety of Ministry of Education (KF201406) and Fundamental Science on Nuclear Safety and Simulation Technology Laboratory, Harbin Engineering University.

References

[1] ISHIDA, I., KUSUNOKI, T., and MURATA, H.: Thermal-hydraulics behavior of a marine reactor during oscillations. Nucl. Eng. Des. , 1990, 120: 213–225.

[2] ISHIDA, I., KUSUNOKI, T., and OCHIAI, M.: Effects by sea wave on thermal hydraulics of marine reactor system. Journal of Nucl. Sci. Tech., 1995, 32: 740–751.

[3] ISHIDA, T., and YORITSUNE, T.: Effects of ship motions on natural circulation of deep sea research reactor DRX. Nucl. Eng. Des. , 2002 215: 51–67.

[4] JAE-HAK K., TAE-WAN K., SANG-MIN L. and *et al.*: Study on the natural circulation characteristics of the integral type reactor for vertical and inclined conditions. 2001, 207: 21–31.

[5] HIROYUKI M., KEN-ICHI S., and MICHIYUKI K.: Experimental Investigation of Natural Convection in a Core of a Marine Reactor in Rolling Motion. Journal of Nuclear Science and Technology, 2000, 37(6): 509-517

[6] HIROYUKI M., KEN-ICHI S., and MICHIYUKI K.: Natural circulation characteristics of a marine reactor in rolling motion and heat transfer in the core. Nuclear Engineering and Design, 2002, 215: 69–85

[7] GAO, P. Z., PANG, F.G., and WANG, Z. X.: Mathematical model of primary coolant in nuclear power plant influenced by ocean condition. J. Harbin Eng. Univ., 1997, 18: 24–27 (in Chinese).

[8] TAN, S.C., SU, G. H., and GAO, P. Z.: Experimental and theoretical study on single-phase natural circulation flow and heat transfer under rolling motion condition. Appl. Therm. Eng., 2009, 29: 3160–3168.

[9] TAN, S. C., SU, G. H., and GAO, P. Z.: Experimental study on two-phase flow instability of natural circulation under rolling motion condition. Ann. Nucl. Energy, 2009, 36: 103–113.

[10] YAN, B. H., YU, L., and LI, Y. Q.: Research on operational characteristics of passive residual heat removal system under rolling motion. Nucl. Eng. Des., 2009, 239: 2302-2310.

[11] YAN B. H., and YU L.: The development and validation of a thermal hydraulic code in rolling motion. Annals of Nuclear Energy, 2011, 38: 1728-1736.

[12] XING D. C., YAN C. Q., and SUN L. C.: Effect of rolling motion on single-phase laminar flow resistance of forced circulation with different pump head. Annals of Nuclear Energy, 2013, 54: 141–148.

[13] MAYINGER F.: Status of thermo-hydraulic research in nuclear safety and new challenges, Eight International Topical Meeting on Nuclear Reactor Thermal-Hydraulics, Kyoto, Japan, 1997.

[14] Leonardo C. R., CHRISTIAN P. M., and Alejandro Clausse. Two-phase flow instabilities: A review. International Journal of Heat and Mass Transfer, 2014, 71: 521–548

[15] ZHANG Y. J., SU G. H., QIU S. Z. and *et al.*: Numerical research on oscillation of two-phase flow in multi-channels under rolling motion. Nuclear Engineering and Design, 2011, 241: 4704-4713

[16] GUO Y., and *et al.*: The influence of ocean conditions on two-phase flow instability in a parallel multi-channel system. Annals of Nuclear Energy, 2008b, 35: 1598-1605.

[17] ROHATGI U. S., NEYMOTIN L.Y., and WULFF W.: Assessment of RAMONA-3B methodology with oscillatory flow tests. Nucl. Eng. Des., 1993, 143(1): 69-82.

[18] Saha M M. A general correlation for heat transfer during film condensation inside pipes [J]. International Journal of Heat and Mass Transfer, 1979, 22: 547-556

[19] LEWIS, E. V.: The Motion of Ships in Waves. Principles of Naval Architecture, 1967, New York.

[20] LEDINEGG M.: Instability of flow during natural and forced circulation, Die Wärme, 1938, 61(8): 891–898.

[21] LU Z.: Two-phase flow and boiling heat transfer, Beijing: Tsinghua University Press, 2002：215-220.(in Chinese)